Proceedings of the 21st ICSMGE, Vienna, Austria, 14 – 19 June 2026. Pistrol, Adam & Schweiger (eds.)
Published by: ÖGG, Austrian Society for Geomechanics, Salzburg, Austria, ISBN 978-3-9503898-4-5
https://doi.org/10.53243/ICSMGE2026-2229

The comprehensive experiments for evaluating the thermomechanical behavior of weathered granite soil taken from Gwangju metro line

Young-Sang Kim
Department of Civil Engineering, Chonnam National University, Gwangju, Republic of Korea, geoyskim@jnu.ac.kr

Hanh Nguyen-Cong, Ju-Won Ryu
Department of Architecture and Civil Engineering, Chonnam National University, Gwangju, Republic of Korea

Gyeong-O Kang
Department of Civil Engineering, Gwangju University, Gwangju, Republic of Korea

Bang Yeon Lee
School of Architecture, Chonnam National University, Gwangju, Republic of Korea

ABSTRACT: Weathered granite soil (WGS) is widely distributed around underground structures in Gwangju, South Korea, and its mechanical response to thermal loading is of particular relevance for energy geostructure applications. This study investigates the thermomechanical behavior of WGS, focusing on volumetric response and shear strength under varying temperatures. A modified temperature-controlled oedometer and a direct shear apparatus were developed to conduct coupled thermomechanical experiments. Volumetric strains in the thermal oedometer tests were analyzed for medium-dense soil under both monotonic and multiple thermal cycles. In addition, this study also evaluated the influence of temperature on soils interface behavior in terms of shear resistance and volumetric deformation during shearing under both dry and saturated conditions. The results indicate that soils undergo irreversible deformation (plastic behavior) after the first heating-cooling cycle. Moreover, accumulated strain occurs after repeated thermal cycles, indicating a thermal hardening behavior similar to that of high-plastic soils. However, the thermal consolidated strain is much smaller than that of high-plasic clay. For the thermal direct shear tests, the soils interface behavior showed insignificant changes in shear strength and volume at the shear plane due to temperature variations for dry soil. However, under saturated conditions, shear resistance exhibited a slight increase with rising temperature, attributed to thermal consolidation of the soil during heating. Nonetheless, the shear strength remained lower than in dry conditions, owing to a reduction in inter-particle interaction under saturation, which resulted in a decreased internal friction angle.

KEYWORDS: Weathered granite soil, thermomechanical behavior, thermal cycles, thermal direct shear test

1 INTRODUCTION

Recently, geothermal heat pump (GHP) systems have been widely adopted by leveraging the high subsurface temperature gradient. For instance, out of approximately 100 GW_{th} of global installed capacity for geothermal heating and cooling, GHPs accounted for about 72 % in 2020, resulting in a 54 % increase from 2015 to 2020 (IRENA, 2023). In South Korea, the total GHP system installed capacity increased from around 250 MW_{th} in 2010 to 1,769 MW_{th} in 2023, largely due to supportive renewable energy policies and government subsidies (Lee and Song, 2024). Generally, vertical GHP systems generally offer higher efficiency due to high subsurface temperature gradient; however, they are costly to install due to deep drilling requirements (Moghanni, Hakkaki-Fard and Hannani, 2023). In contrast, horizontal systems are more cost-effective but require large land areas and are less thermal efficient in temperature changes (Kim et al., 2023). To address these drawbacks, energy geostructures (EGS) have recently been proposed by integrating GHP energy pipes into underground structures such as retaining walls, tunnels, basement slabs, and pile foundations (Laloui and Rotta Loria, 2020; Meibodi and Loveridge, 2022). This approach not only reduces installation costs but also enhances heat transfer efficiency due to the deeper placement of these systems compared to horizontal GHPs. However, during the operation of energy geostructures, heat is transferred to the surrounding walls and ground, leading to changes in the mechanical behavior of ground, including volume change and variations in the sheer strength of soil under thermal loading.

The thermal volumetric change has been recently investigated for pure clay and clean sand using thermal triaxial test and oedometer test. Fine-grained soils such as clays show complex thermal behavior strongly influenced by factors like overconsolidation ratio (OCR) (Laloui and Rotta Loria, 2020). Early studies on various clays revealed that normally consolidated (NC) clays typically undergo irreversible thermal contraction, while overconsolidated (OC) clays exhibit reversible volumetric expansion during heating (Azhar et al., 2024). Slightly OC soils may initially expand and then contract (Laloui and Di Donna, 2013). Notably, heating reduces pore water viscosity and dielectric constant, weakening inter-particle forces and promoting water dissipation and particle rearrangement, which leads to densification in NC soils (Golchin, Vardon and Hicks, 2022). In contrast, OC soils resist such rearrangement due to prior stress history, resulting mainly in thermoelastic expansion.

Thermally induced volumetric strain of saturated coarse-grained soil is also investigated in previous studies (Ng et al. 2016, Sittidumrong et al. 2019). The observation indicates that the volumetric change in coarse-grained soil strongly depends on relative density and stress variations. Loose sand generally shows an initial contraction at the beginning of heating, which then transforms into expansion once the temperature becomes sufficiently high, whereas dense sand exhibits significant expansion throughout the heating stage (Rotta Loria and Coulibaly, 2021). However, most of these studies focus on investigating the mechanical responses of uniform soils with low fine content. The soil-soil and soil-structure interfaces behavior under temperature effect are widely presented for clean sand and pure clay (Di Donna, Ferrari and Laloui, 2016; Maghsoodi, Cuisinier and Masrouri, 2020). The soil-soil interface behavior under dry conditions were unaffected by temperature variations.

This study aims to comprehensively evaluate the thermomechanical behavior of weathered granite soil (WGS) collected from the Gwangju metro line through a series of laboratory tests, including modified thermal oedometer and thermal direct shear tests. The volumetric strain and shear resistance responses of WGS, characterized by relatively high fine content and low plasticity, are investigated in a medium-dense state under both dry and saturated conditions.

2 EXPERIMENTAL PROGRAM

2.1 *Tested materials*

Undisturbed and disturbed weathered granite soil (WGS) samples were collected near Gwangju Metro Lines 1 and 2 in the Gwangju region, South Korea. These samples were carefully extracted to capture both the in-situ structure of the intact material and the remolded condition of the disturbed soil. The general properties of the WGS and their particle size distribution curves were determined in the laboratory, as shown in Figure 1 and summarized in Table 1.

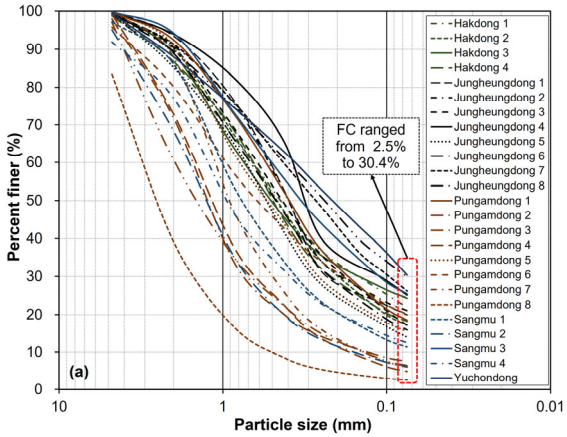

Figure 1. Particle size distribution curve of WGS

Table 1. Soil properties

Parameter	Symbol	Value		Unit
		Jeunghung	Yuchon	
Coefficient of uniformity	C_u	21.9	20.6	-
Specific gravity	G_s	2.650	2.645	-
Max. void ratio	e_{max}	1.453	1.118	-
Min. void ratio	e_{min}	0.547	0.556	-
Water content	w	23.7	22.8	%
Liquid limit	LL	37	-	%
Plastic index	PI	2.6	-	%
Fine content	-	29.8	30.4	%
Classification	-	SM	SM	-

The results show that WGS has a wide range of fine content, varying from 2.5 % to 30.4 %, reflecting the heterogeneous nature of weathered granite deposits and the varying degrees of mineral decomposition. As illustrated in Figure 1, most soil samples are classified as silty sand (SM) with relatively high fine content. Table 1 also shows that the liquid limit and plasticity index classify the soil as low-plasticity, differing from previous studies that focused on pure clays with high plasticity (Delage, Sultan and Cui, 2000; Trani, Bergado and Abuel-Naga, 2010) . In addition, based on the distribution curve, the WGS exhibits a more well-graded distribution compared to earlier studies on clean sands (uniformly graded sands) (Ng, Wang and Zhou, 2016; Sittidumrong, Jotisankasa and Chantawarangul, 2019).

2.2 *Tested equipment*

The modified thermal oedometer and direct shear equipment were conducted for evaluating volumetric strain and shear resistance of WGS under thermal loading. Figure 2 demonstrates that modified thermal oedometer setup integrates a conventional mechanical loading frame with a thermal programmable water bath (-25 °C to 150 °C, Jeio Tech Co., Ltd.) controlled via PID. Vertical load is applied by dead weights, and displacement is measured by a digital dial gauge (0.001 mm resolution), recorded automatically. The soil specimens (2×6 cm) are indirectly heated and cooled through three layers: circulating water, an aluminum plate, and static distilled water in contact with the sample.

The configuration of the thermal direct shear test is shown in Figure 3. The heat transfer procedure is similar to that used in the thermal oedometer test, where the soil is indirectly heated through layers of materials such as stainless steel and porous stone in vertical arrangement, ensuring a sequential heat transfer mechanism like the field conditions around energy geostructures. However, in this test, the normal load is applied by a program at a constant loading rate.

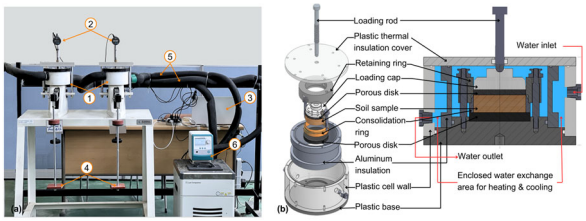

Figure 2. (a) Experiment setup of modified thermal oedometer test: 1-modified cells; 2-dial gauges; 3-data logger; 4-applied load; 5-heat transform water tube; 6-water bath for heating and cooling, (b) Structure of modified thermal oedometer cell.

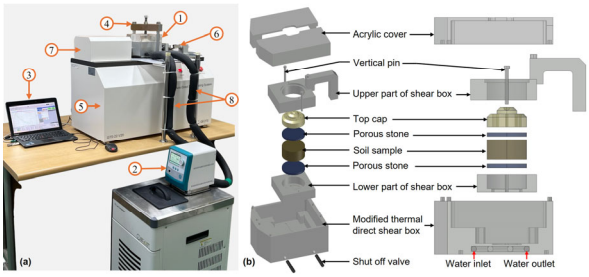

Figure 3. (a) Configuration of test equipment: 1-modified thermal direct shear box; 2-water bath for heating/cooling process; 3-acquisition and reading program; 4-top crossbar; 5-normal actuator in direct shear device; 6-load cell; 7-horizontal actuator; 8-tubes transferring circulating water, (b) Structure of modified thermal direct shear box.

2.3 *Equipment calibration*

Thermally induced volumetric changes that measures in thermal oedometer test and thermal direct shear test may reflect not only soil deformation but also the thermal response of the device components, such as the metal ring, porous stone, top cap, and loading rod (Abuel-Naga, Bergado and Bouazza, 2007). To isolate the actual soil strain, the thermal deformation of the apparatus was carefully calibrated and removed from the recorded displacement.

The actual axial strain of soil is given by:

$$\varepsilon_{zT}^{s} = \varepsilon_{zT}^{m} - \varepsilon_{zT}^{eq.} = \varepsilon_{zT}^{m} - (\varepsilon_{zT}^{t} + \varepsilon_{zT}^{r}) \quad (1)$$

where ε_{zT}^{s} is the axial strain of soil, ε_{zT}^{m} is measurement axial strain, ε_{zT}^{t} is measurement strain of top component, ε_{zT}^{r} is equivalent axial strain of soil due to radial expansion of ring during thermal loading.

Notably, as temperature increases, the metal ring tends to expand outward, creating a slight gap between the soil and the ring wall. This allows the soil to deform laterally into space, resulting in an apparent reduction in vertical height. The relationship between lateral expansion and the corresponding vertical strain can be represented using the Poisson ratio of soil. Based on Hooke's law, the axial strain increment is given by equation as below:

$$\Delta\varepsilon_z = \frac{1}{E}\left[\Delta\sigma_z - \nu\left(\Delta\sigma_x + \Delta\sigma_y\right)\right] \quad (2)$$

Under constant stress during thermal loading, i.e., $\Delta\sigma_z = 0$ and $\Delta\varepsilon_{xT} = \Delta\varepsilon_{yT} = \Delta\varepsilon_{rT}$, Equation 2 can be rewritten as follows:

$$\Delta\sigma_z = \frac{\nu E(\Delta\varepsilon_{zT}^{r} + 2\Delta\varepsilon_{rT})}{(1+\nu)(1-2\nu)} + \frac{E}{1+\nu}\Delta\varepsilon_{zT}^{r} \quad (3)$$

$$\Delta\varepsilon_{zT}^{r} = -\frac{2\nu}{1-\nu}\Delta\varepsilon_{rT} \quad (4)$$

where $\Delta\varepsilon_{rT}$ is the radial strain increment of soil during thermal loading, assuming that the radial deformation of the soil is approximately similar to that of the ring due to their relative small strain and nearly identical Poisson's ratios of 0.3.

By combining Equation (1) and (4), the thermal volumetric strain during thermal loading can be expressed as:

$$\varepsilon_{vT} = \varepsilon_{zT}^{s} + 2\varepsilon_{rT} = \varepsilon_{zT}^{m} - \varepsilon_{zT}^{t} + \frac{2}{1-\nu}\varepsilon_{rT}^{r} \quad (5)$$

2.4 *Experimental procedures*

For thermal oedometer test, experiments were conducted on both disturbed and undisturbed saturated samples of Jeunghung (Jh) soil. For undisturbed samples, the thermal consolidation of was carried out in two stages: 1-heating from 20 °C to 60 °C with heating rate of 3 °C/h, and 2-applying mechanical loading under a constant temperature of 60 °C. This test series is referred to as Jh.TCO60 (Table 2) and was compared with a conventional consolidation oedometer test (Jh.CCO) conducted at 20 °C. Thermal cycles were also employed for disturbed soil samples under different of normal effective stress of 40 kPa, 320 kPa, and 640 kPa with relative density of 60 %. The heating rate of 3 °C/h and cooling rate of 5 °C/h were imposed to minimize the pore water pressure generation during heating (Di Donna and Laloui, 2015; Hoseinimighani, Tourchi and Szendefy, 2023). These case studies schedules of Jh.Dr60.40, Jh.Dr60.320, and Jh.Dr60.640 are detailed in Figure 4(a) and Table 2 (upper part).

In the case of the thermal direct shear test, Yuchon soil was selected to evaluate the influence of temperature on both shear strength and volumetric changes under dry and saturated conditions, each prepared at a relative density of 60 %. The testing program was designed to capture the coupled thermo-mechanical response of the soil at the soil-soil interfaces. As illustrated in Figure 4(b), the procedure consisted of three main stages: 1-applying normal stress, 2-increase temperature to setting values with heating rate of 5 °C/h (saturated state) and 20 °C/h (dry condition), and 3- applying the shear force until the desired displacement or failure condition was reached. A total of 18 thermal direct shear test cases were carried out, as summarized in the lower part of Table 2, covering a range of temperature levels, normal stresses, and saturation states.

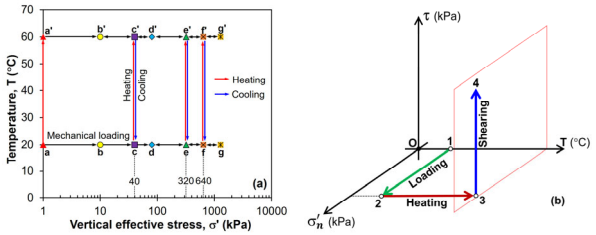

Figure 4. Experiment procedure of: (a) thermal oedometer test, (b) thermal direct shear test.

Table 2. Experimental case studies

Case study	Stress path	Normal stress, σ_n' (kPa)	Temperature change, T (°C)
Jeunghung soil (Thermal Oedometer)			
Jh.Dr60.40	a→c→c′→c	1→40	20→60→20
Jh.Dr60.320	a→e→e′→e	1→320	20→60→20
Jh.Dr60.640	a→f→f′→f	1→640	20→60→20
Jh.CCO	a→g→d	1→1280→80	20
Jh.TCO60	a→a′→g′→b′	1→1280→10	20→60
Yuchon soil (Thermal direct shear)			
YC.dry.50	1→2→3→4	1→50	{20, 40, 60}
YC.dry.100	1→2→3→4	1→100	{20, 40, 60}
YC.dry.150	1→2→3→4	1→150	{20, 40, 60}
YC.sat.50	1→2→3→4	1→50	{20, 40, 60}
YC.sat.100	1→2→3→4	1→100	{20, 40, 60}
YC.sat.150	1→2→3→4	1→150	{20, 40, 60}

3 RESULTS AND DISCUSSION

3.1 *Thermally induced volumetric change*

Thermal volumetric strain behavior of Jeunghung soil under different vertical stresses and thermal cycles are illustrated in Figure 5. Figure 5a compares the thermal volumetric response during the first heating cycle under various vertical stresses (40, 320, and 640 kPa). All samples exhibit contractive behavior with increasing temperature and the magnitude of contraction decrease with higher vertical stress. For instance, at 60 °C, the sample under 40 kPa shows the largest thermal volumetric strain (0.4 %), followed by the 320 kPa (0.27 %) and 640 kPa (0.25 %) cases. This reduced thermal contraction at higher vertical stresses is probably attributed to the denser soil structure and stronger inter-particle contacts, which decrease the potential rearrangement during heating. In contrast, soils under lower stress remain relatively loose, allowing more particle rearrangement and resulting in greater thermal contraction (Di Donna and Laloui, 2015). Notably, the difference in strain between 320 and 640 kPa is relatively small, suggesting that thermal contraction tends to converge at higher stress levels.

Figures 5(b)–(d) present the evolution of thermal volumetric strain under multiple heating-cooling cycles at vertical stresses of 40 kPa, 320 kPa, and 640 kPa, respectively. For all stress levels, the volumetric contraction accumulates progressively with each thermal cycle, especially in the early cycle, as shown in the Figure 6. However, the strain increment per cycle reduces with repeated cycling, indicating a tendency toward thermal stabilization. Besides, the slope of the cooling curves exhibits the unchange under different vertical stresses and cycles,

indicating the thermoelastic deformation during cooling progress (Yao and Zhou, 2013; Laloui and Rotta Loria, 2020; Ng et al., 2024).

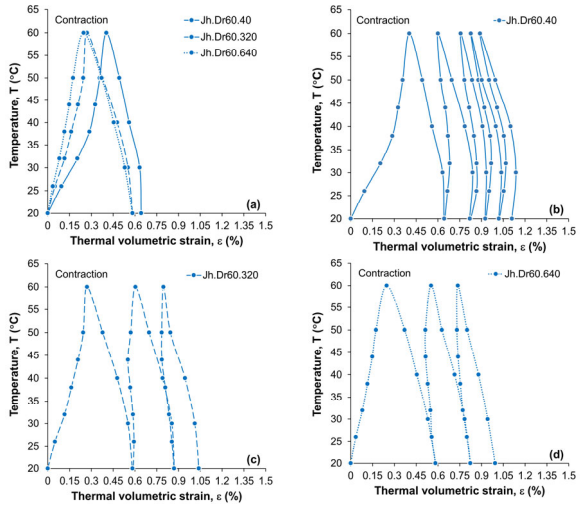

Figure 5. Thermal cycles effect on volumetric strain (a) strain due to first thermal cycle; (b)-(d) strain due to multiple thermal cycles.

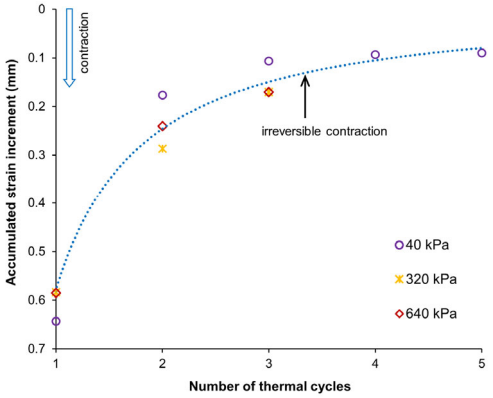

Figure 6. Accumulated strain increments of WGS during thermal cycles.

Figure 7 indicates that weathered granite soil, with a very low plasticity index (PI =2.6) exhibits significantly smaller accumulated volumetric strain per thermal cycle compared to high-plasticity clays. The normalized strain ($\Delta\varepsilon/\Delta T$) of WGS ranges from 0.006 to 0.01 %/°C, whereas high-plasticity clays (PI > 17 (Murthy, 2007)) typically show values upto 0.08 %/°C. Quantitatively, this means that highly plastic clays heating strain is significantly larger than WGS under similar temperature ranges. Notably, high-plasticity soils contain greater amounts of clay minerals, particularly active clays such as montmorillonite. For example, Bangkok clay (PI = 60) contains approximately 54% to 71% smectite (Abuel-Naga et al., 2007), while Boom clay (PI = 50) contains about 33% (Yu et al., 2012). These minerals contain large specific surface areas and thicker adsorbed and diffuse double water layers, both of which are highly sensitive to temperature. Heating alters these interactions by increasing molecular kinetic energy, reducing the dielectric permittivity of water, and accelerating ion mobility. These changes promote desorption of strongly bound water, compression of the diffuse double layer, and weakening of physicochemical particle contacts (Azhar et al., 2024). Consequently, the irreversible contraction observed in normally consolidated high-plasticity clays has been significantly attributed to temperature-induced changes in the adsorbed water layer and the diffuse double layer. Consistently, the thickness of the bound water layer has been reported to decrease with increasing temperature (Zymnis, Whittle and Germaine, 2019).

On the other hand, the thermal contraction observed in granular soils is primarily driven by thermal-induced adjustments of the soil skeleton and particle rearrangement, partly distinct from the physicochemical effects dominant in high plasticity clays. The thermal volumetric contraction in granular soil is primarily caused by the thermal expansion of solid particles, which tightens inter-particle contacts and triggers grain rearrangement (Ng, Wang and Zhou, 2016). In addition, free pore water exhibits a much larger thermal expansion than soil solids and, due to its decreasing viscosity at higher temperatures, dissipates more easily. This accelerated dissipation process alters the soil skeleton structure, leading to irreversible plastic contraction.

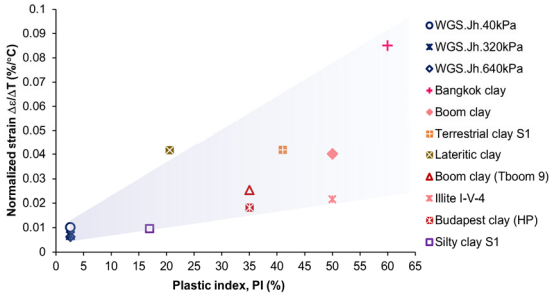

Figure 7. Plasticity-dependent thermal hardening of different soils: WGS compared to Bangkok clay (Abuel-Naga et al., 2007), Boom clay (Baldi, Hueckel and Pellegrini, 1988; Sultan, Delage and Cui, 2002), Terrestrial clay(Shetty, Singh and Ferrari, 2019), Lateric clay (Xu, Chen and Xia, 2024), Illite (Campanella and Mitchell, 1968), Budapest clay (Mighani et al., 2025), Silty clay (Di Donna and Laloui, 2015).

3.2 *Influence of temperature on soil-soil interface behavior*

3.2.1 *Dry state*

Figure 8 illustrates the shear stress-horizontal displacement and volumetric deformation during the shear test of Yuchon WGS under different temperatures (20 °C, 40 °C, and 60 °C) in dry conditions for three normal stress levels. The results indicate that under three normal stress levels of 50 kPa, 100 kPa, and 100 kPa, the shear strength remains mostly unchanged with increasing temperature, which is consistent with previous studies (Di Donna, Ferrari and Laloui, 2016).

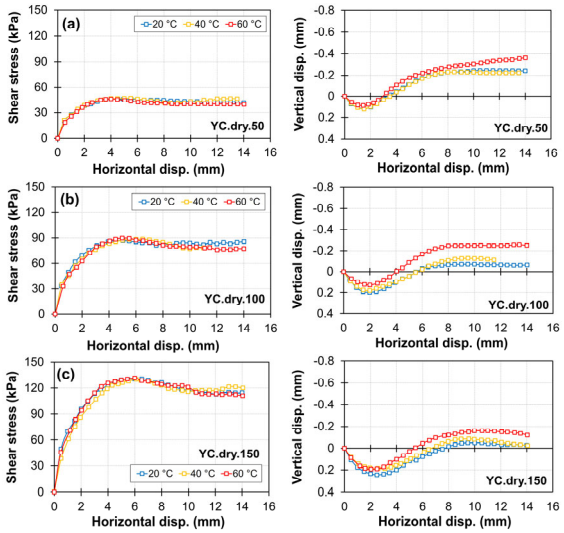

Figure 8. Direct shear test results of dry WGS under thermal loading.

With a medium-dense soil state (relative density of 60 %), the soil initially exhibits contraction at the beginning of the shear test due to the applied vertical stress, which causes particle rearrangement contraction. As the test progresses, the soil reaches a denser state and subsequently begins to dilate, i.e., its volume increases. Besides, at the highest temperature (60 °C), the volumetric dilation response exhibits a relatively small increase compared to 20 and 40 °C under all three normal stress conditions.

3.2.2 *Saturated state*

Figure 9 presents the shear stress-displacement and volumetric responses of Yuchon WGS under thermal loading in saturated conditions. At all normal stress levels, the shear stress increases rapidly with horizontal displacement and finally maintains a nearly constant value. Unlike dry state, compared with the lower temperatures (20 °C and 40 °C), specimens tested at 60 °C tend to exhibit slightly higher shear resistance, particularly at 100 kPa and 150 kPa. In terms of volumetric behavior, soils under 50 kPa and 100 kPa show initial contraction followed by a tendency toward dilation at 60 °C, while tests at 150 kPa remain largely contractive throughout the shearing process. Notably, with increase of normal stress, the shear stress-horizontal displacement and volumetric behaviors resemble the typical response of loose soils, which show a smooth increase in shear stress before stabilizing at the critical state, while volumetric contraction dominates during shearing. This behavior is probably explained by the presence of pore water, which may reduce inter-particle friction between soils interface, thereby weakening the soil skeleton interaction compared with the dry state (Figure 8). In addition, thermal effects may generate pore water pressure, resulting in a slight decrease in effective stress, further reducing shear strength as shown in Figure 9.

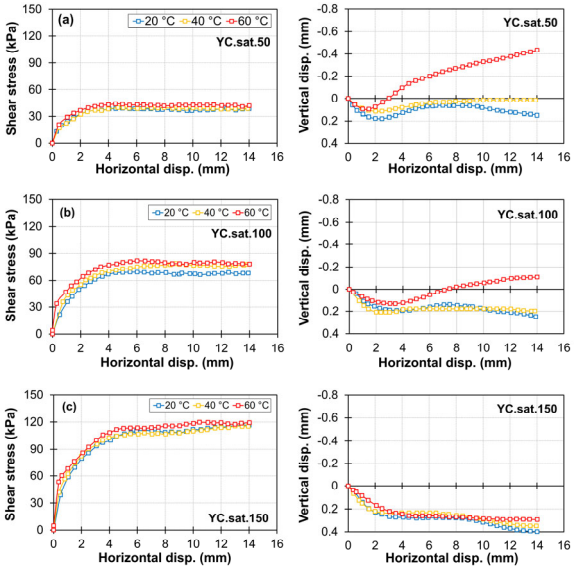

Figure 9. Direct shear test results of saturated WGS under thermal loading.

3.2.3 *Internal friction angles and dilatancy angles*

As mentioned in the previous study, the influence of temperature on the direct shear test under dry conditions is negligible. It is clearly shown that the internal friction angle remains mostly unchanged with increasing temperature, as illustrated in Figure 11(a). In contrast, these values slightly increase under saturated conditions. This is attributed to thermal consolidation occurring during the temperature increase in the saturated state (Maghsoodi, Cuisinier and Masrouri, 2020). Indeed, Fig. 11 shows that the volume of the soil sample tends to consolidate at the end of the heating stage, thereby increasing the particle-interaction surface within the soil structure. This observation is consistent with the conclusions obtained from the thermal oedometer experiments. However, despite this slight increase, the internal friction angle in the wet case remains smaller than that of the dry state, as shown in Figure 10(b), resulting in a slight decrease in shear strength for the saturated soil (Figure 8 and 9).

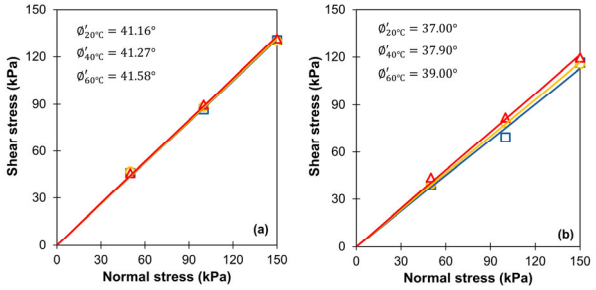

Figure 10. Internal friction angle at: (a) dry (b) saturated conditions.

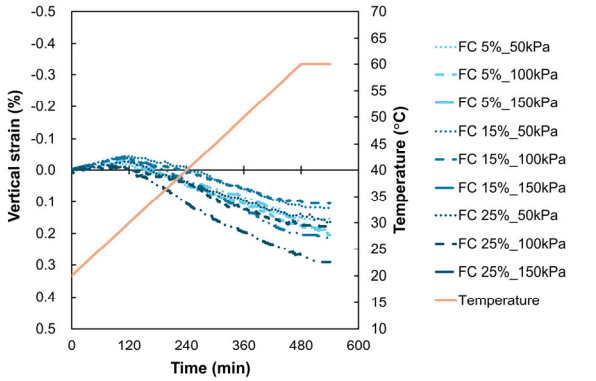

Figure 11. Thermal consolidated strain during heating of soils.

The volumetric change is also explained by the dilatancy angles. In Figure 12, the dilatancy behavior of weathered granite soil is compared under dry and saturated conditions. Under dry conditions, the soil exhibits pronounced positive dilatancy angles i.e., soil expands in volume during shearing, with peak values that increase as vertical stress and temperature increase. In contrast, saturated specimens show much lower dilatancy peaks and significant negative dilatancy angles, indicating that the soil transitions toward contraction, as shown in Figure 8.

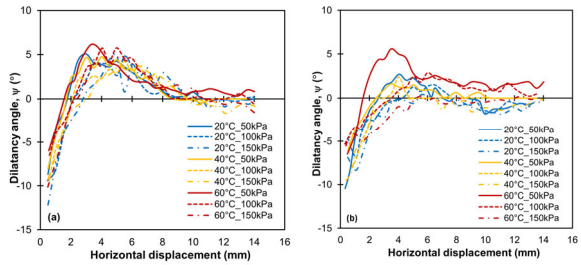

Figure 12. Dilatancy angle at: (a) dry (b) saturated conditions.

4 CONCLUSIONS

This study comprehensively evaluated the thermomechanical behavior of weathered granite soil (WGS) collected from the Gwangju metro line through a series of laboratory tests, including modified thermal oedometer and thermal direct shear tests. The WGS is classified as silty sand with relatively high fine content and low plasticity. The main conclusions are as follows:

i. Thermal oedometer tests show irreversible contraction in WGS that depends on vertical effective stress. Repeated heating–cooling leads to accumulated strain, indicating thermal hardening behavior. Lower normal stresses allow higher potential contractive deformation during heating, while volumetric strain differences at higher stresses remain relatively small.

ii. WGS exhibits minimal thermally induced volumetric strain compared with clay, highlighting the strong control of mineralogy and plasticity on thermal sensitivity. In contrast, high-plasticity clays, rich in active minerals, undergo much larger thermal contraction due to thermal-induced changes in bound-water thickness and diffuse double-layer compression.

iii. Temperature also affects soils shear strength in saturated condition due to thermal consolidation, resulting in a slightly increases shear resistance. Nevertheless, saturated strengths remain lower than dry strengths because interparticle interactions weaken and the internal friction angle decreases.

5 ACKNOWLEDGEMENTS

This work was supported by the National Research Foundation of Korea (NRF) grant funded by the Korea government (MSIT) (RS-2025-00512551 and RS-2025-00518115).

6 REFERENCES

Abuel-Naga, H.M., Bergado, D.T. and Bouazza, A., 2007. Thermally induced volume change and excess pore water pressure of soft Bangkok clay. *Engineering Geology*, 89(1–2), pp.144–154. https://doi.org/10.1016/j.enggeo.2006.10.002.

Azhar, M., Mondal, S., Tang, A.M. and Singh, A.K., 2024. Effect of temperature on the mechanical properties of fine-grained soils - A review. *Geothermics*, [online] 116(October 2023), p.102863. https://doi.org/10.1016/j.geothermics.2023.102863.

Delage, P., Sultan, N. and Cui, Y.J., 2000. On the thermal consolidation of Boom clay. *Canadian Geotechnical Journal*, 37(2), pp.343–354. https://doi.org/10.1139/cgj-37-2-343.

Di Donna, A., Ferrari, A. and Laloui, L., 2016. Experimental investigations of the soil–concrete interface: Physical mechanisms, cyclic mobilization, and behaviour at different temperatures. *Canadian Geotechnical Journal*, 53(4), pp.659–672. https://doi.org/10.1139/cgj-2015-0294.

Di Donna, A. and Laloui, L., 2015. Response of soil subjected to thermal cyclic loading: Experimental and constitutive study. *Engineering Geology*, [online] 190, pp.65–76. https://doi.org/10.1016/j.enggeo.2015.03.003.

Golchin, A., Vardon, P.J. and Hicks, M.A., 2022. A thermo-mechanical constitutive model for fine-grained soils based on thermodynamics. *International Journal of Engineering Science*, 174, p.103579. https://doi.org/10.1016/J.IJENGSCI.2021.103579.

Hoseinimighani, H., Tourchi, S. and Szendefy, J., 2023. Thermomechanical behaviour of silty sandy clays: An experimental and numerical investigation. *International Society for Soil Mechanics and Geotechnical Engineering*, [online] 1(2), pp.161–162. https://doi.org/10.53243/NUMGE2023-380.

IRENA, 2023. *Global geothermal: market and technology assessment - International Renewable Energy Agency*.

Kim, Y.S., Dinh, H.B., Kang, G.O. and Hoang, D.T., 2023. Performance evaluation of a novel horizontal ground heat exchanger: Coil-column system. *Journal of Building Engineering*, 76, p.107180. https://doi.org/10.1016/J.JOBE.2023.107180.

Laloui, L. and Di Donna, A., 2013. *Energy Geostructures: Innovation in Underground Engineering*.

Laloui, L. and Rotta Loria, A.F., 2020. *Analysis and Design of Energy Geostructures - Theoretical Essentials and Practical Application*.

Lee, T.J. and Song, Y., 2024. IEA Geothermal: 2023 Republic of Korea Country Report. (May).

Maghsoodi, S., Cuisinier, O. and Masrouri, F., 2020. Thermal effects on mechanical behaviour of soil–structure interface. *Canadian Geotechnical Journal*, [online] 57(1), pp.32–47. https://doi.org/10.1139/cgj-2018-0583.

Meibodi, S.S. and Loveridge, F., 2022. The future role of energy geostructures in fifth generation district heating and cooling networks. *Energy*, [online] 240, p.122481. https://doi.org/10.1016/J.ENERGY.2021.122481.

Moghanni, R., Hakkaki-Fard, A. and Hannani, S.K., 2023. A comprehensive study on the performance of vertical ground-coupled heat pumps. *Geothermics*, [online] 110, p.102674. https://doi.org/10.1016/J.GEOTHERMICS.2023.102674.

Ng, C.W.W., Wang, S.H. and Zhou, C., 2016. Volume change behaviour of saturated sand under thermal cycles. *Geotechnique Letters*, 6(2), pp.124–131. https://doi.org/10.1680/jgele.15.00148.

Ng, C.W.W., Zhao, X., Zhang, S. and Zhang, Q., 2024. A unified thermo-mechanical bounding surface model for saturated clay and sand. *Computers and Geotechnics*, [online] 173(January), p.106535. https://doi.org/10.1016/j.compgeo.2024.106535.

Rotta Loria, A.F. and Coulibaly, J.B., 2021. Thermally induced deformation of soils: A critical overview of phenomena, challenges and opportunities. *Geomechanics for Energy and the Environment*, [online] 25, p.100193. https://doi.org/10.1016/j.gete.2020.100193.

Sittidumrong, J., Jotisankasa, A. and Chantawarangul, K., 2019. Effect of thermal cycles on volumetric behaviour of Bangkok sand. *Geomechanics for Energy and the Environment*, 20, p.100127. https://doi.org/10.1016/J.GETE.2019.100127.

Trani, L.D.O., Bergado, D.T. and Abuel-Naga, H.M., 2010. Thermo-mechanical behavior of normally consolidated soft Bangkok clay. *International Journal of Geotechnical Engineering*, 4(1), pp.31–44. https://doi.org/10.3328/IJGE.2010.04.01.31-44.

Yao, Y.P. and Zhou, A.N., 2013. Non-isothermal unified hardening model: A thermo-elasto-plastic model for clays. *Geotechnique*, 63(15), pp.1328–1345. https://doi.org/10.1680/geot.13.P.035.